Author(s): Lindgren, Juuso & Niemi, Rami & Lund, Peter D.

Title: Effectiveness of smart charging of electric vehicles under power limitations

Year: 2013

Version: Post print

Please cite the original version:

Lindgren, Juuso & Niemi, Rami & Lund, Peter D. 2013. Effectiveness of smart charging of electric vehicles under power limitations. International Journal of Energy Research. Volume 38, Issue 3. P. 404-414. ISSN 0363-907X (printed). DOI: 10.1002/er.3130.

Effectiveness of smart charging of electric vehicles under power limitations

Juuso Lindgren, Rami Niemi, and Peter D. Lund
New Energy Technologies Group
Aalto University, School of Science
P.O. Box 14100, FI-00076 Aalto (Espoo), Finland
e-mail: peter.lund@aalto.fi

Summary

This article investigates charging strategies for plug-in hybrid electric vehicles (PHEV) as part of the energy system. The objective was to increase the combined all-electric mileage (total distance driven using only the traction batteries in each PHEV) when the total charging power at each workplace is subject to severe limitations imposed by the energy system. In order to allocate this power optimally, different input variables, such as state-of-charge, battery size, travel distance, and parking time, were considered. The required vehicle mobility was generated using a novel agent-based model that describes the spatiotemporal movement of individual PHEVs. The results show that, in the case of Helsinki (Finland), smart control strategies could lead to an increase of over 5% in the all-electric mileage compared to a no-control strategy. With a high prediction error, or with a particularly small or large battery, the benefits of smart charging fade off. Smart PHEV charging strategies, when applied to the optimal allocation of limited charging power between the cars of a vehicle fleet, seem counterintuitively to provide only a modest increase in the all-electric mileage. A simple charging strategy based on allocating power to PHEVs equally could thus perform sufficiently well. This finding may be important for the future planning of smart grids as limiting the charging power of larger PHEV fleets will sometimes be necessary as a result of grid restrictions.

Keywords: batteries, plug-in hybrid electric vehicles, electric vehicles, power grids, smart control, smart grids

Nomenclature

A	Attraction function
c	Unit electricity consumption of a vehicle (kWh·km^{-1})
d	Distance (km)
dt	Time step or interval (s)
D	Next free distance (km)

E	Energy (kWh)
i, j, n	Node
N	Number of vehicles assigned to a certain node
P	Power (MW)
Q	Battery capacity (kWh)
r	Random number
s	Saturation factor
S	Saturation function
SOC	State-of-charge (kWh)
$\widehat{\mathrm{SOC}}$	Normalized state-of-charge
t	Time (time steps)
$\bar{t}$	Mean time (time steps)
T	Remaining parking time (time steps)
$\bar{T}$	Mean remaining parking time (time steps)
u	Fitness (km^{-1})
v	Vehicle
V	Group of vehicles at a certain node
w	Normalized weight
x	Percentage of vehicles to be saturated
Z	Charging function
δ	Error parameter
η	Power transfer efficiency
σ	Free parameter

Subscripts

0	Exactly known
A	Arrival
D	Departure
i, j	Node
T	Timer
$\max$	Maximum
t	Time step
v	Vehicle
x	Percentage of vehicles to be saturated

Superscripts

A, B, C	Battery charging strategies
socket	Charging socket energy transfer limitation during one time step
step	Battery energy transfer limitation during one time step

Abbreviations

EV	Electric vehicle
PHEV	Plug-in hybrid electric vehicle
SOC	State-of-charge
V2G	Vehicle-to-grid operation of electric vehicle

1. Introduction

The transport sector is responsible for 25% of global CO_2 emissions, a figure driven upwards by the increasing mobility demand of emerging economies. Three-quarters of these emissions are attributable to cars and trucks [1]. As half of all oil is consumed by the transport sector, the price of oil and the adequacy of its supply raise major concerns as well [2]. Energy security and climate change mitigation are compelling drivers to develop alternatives, such as electric mobility [3]–[5], to conventional transportation. However, the impact of the alternative technologies has remained minor because of the high associated costs. Policy measures, such as fuel taxes and vehicle investment subsidies, may be necessary to make these technologies an economic alternative for the consumer [6],[7].

Assuming that appropriate policies are introduced, electric vehicles (EVs) are likely to become more prevalent. This presents both challenges and opportunities for the operation of the power grid. Specifically, with a high EV penetration the grid may become overloaded if their charging is left uncontrolled [5],[8],[9]. On the other hand, EVs can provide demand-side management options for power profile leveling [10] or to minimize power losses in general [11]. Several authors have suggested vehicle-to-grid (V2G) strategies to balance variable renewable generation [8],[9],[12], particularly wind power [8],[13],[14], but these strategies may need to be viewed critically in terms of increased battery degradation [15]–[17]. In addition to consumption and production leveling, EVs are also capable of providing other ancillary services, such as frequency regulation [18]. Smart EV control strategies may not only improve their technical quality as part of the grid, but also yield considerable economic benefits [19]. For example, the electricity price can be used for the control of EV battery charging in order to benefit from the inexpensive electricity that is available [20].

Therefore, charging control (and discharging in the case of V2G) is a crucial theme for both the utility of EV mobility and its smooth integration into the electricity system. This control may influence several qualities, such as the operational range of EVs, the power levels involved [21],[22], the running energy costs of the EV, and the trade-offs between battery capacity and power management [23]–[25].

Studies on EV charging control can be roughly divided into two categories: energy allocation and power allocation. In energy allocation studies, the timing of charging is examined and optimized for one time period, usually one day. The relevant question is: where and how should the EV load be placed in time to obtain the most favorable combined load profile, e.g., one that minimizes total energy generation

costs? Studies on optimal energy allocation are abundantly available; for recent publications, see e.g., [26]–[28]. Power allocation studies, on the other hand, investigate the charging separately at each time point. The question here is how the available power should be allocated to the connected vehicles to obtain the best result, e.g., the highest average state-of-charge (SOC). The difference between energy and power allocation could also be interpreted as follows: the energy allocation solves one large problem at once, while the power allocation solves several smaller problems in succession.

The current study resides in the power allocation category. It examines charging control strategies under power limitations that arise from grid stability requirements. The problem of optimal charging power allocation has been studied using various approaches, including game theory and evolutionary optimization [20],[29],[30]. These studies have used e.g., the target SOC, the remaining expected parking time, and the electricity price as inputs to the allocation algorithm. The objective functions have ranged from maximizing the average (normalized) SOC to maximizing the utility, or the value an EV owner places on the electricity they have received. However, the total traffic electrification (here measured by the combined all-electric mileage) as the maximization objective has thus far been largely ignored. Furthermore, prediction errors should always be considered, as their magnitude is often linked to the effectiveness of sophisticated charging strategies. Thus, the current study investigates several allocation strategies that attempt to increase the all-electric mileage, employing both known and unknown (predicted) parameters as inputs. It also examines the effect of prediction errors, along with changes in battery capacity, and compares all these strategies against the simple equal allocation method.

A novel modeling approach, essentially an agent-based PHEV trip generation algorithm, is applied to provide the mobility necessary for studying the different strategies. The algorithm generates a detailed spatial and short time interval (5 min) description of the movement of a large EV fleet on a single-vehicle level within the road network, leading to a spatio-temporal distribution of EV power demand. Previous studies have employed aggregated or integrated methods of modeling EV mobility [20],[31], but there are also studies with remarkably detailed spatio-temporal modeling [32],[33]. The model presented here can be considered to lie between these extremes in the complexity range.

2. Modeling of EVs in the energy system

There are two main approaches for modeling the interaction between EVs and the energy system. The first approach has its focus on the *cause* (EV traffic), while the other focuses on the *effects* (energy

traffic).

Effect-based models consider EVs in an aggregated way without specifically modeling the spatial movement of the vehicles, e.g., by using empirical travel data or statistical models [23],[31],[34]. In an aggregated model, EV charging or discharging is basically an interaction of a dynamic electric storage with the grid [31].

An alternative is to model the physical movement of the EVs. Such agent-based approaches may employ partial tracking of the EV location, e.g., by aggregating individual EVs into several EV fleets, or highly detailed spatio-temporal modeling of single vehicles [32]. Agent-based models yield information on vehicles' location and parking times, which is essential when trying to assess their energy system impacts accurately. On the other hand, these models tend to be much more complex and require more computation time than the aggregated methods.

In this study, we employ a simple agent-based model that is capable of describing the movement of single vehicles within a larger fleet. To avoid having to include social range anxiety effects in the model, only plug-in hybrid electric vehicles (PHEV) are considered. The main input data required fall within the following five categories and will be explained in greater detail later: 1) PHEV-specific parameters; 2) road and grid network topology; 3) travel patterns and distances; 4) Charging infrastructure, and 5) PHEV control.

The main output from the model contains the spatial and temporal distributions of the movement and power impacts of PHEVs. The algorithm is explained in more detail below.

2.1 Node network

Figure 1 illustrates the node network approach used in the study. The urban area is divided into several zones, each represented by a node. Each node can have one of four different types based on the "main activity" in the area. The labels of the different node types are: home (1), work (2), shop (3), and leisure (4). These nodes can be linked with the electric grid in an arbitrary way.

For the current analysis, a road network for Helsinki, Finland, was created. It is based on street/road infrastructure data from Google Maps [35]. In this network, the city is divided into 288 zones, or nodes, representing the main car parking locations. After this, one of the four types was assigned to the majority of the nodes on the basis of our understanding of the area. Finally, the Dijkstra algorithm was used to

calculate the distances between all the node pairs [26]. The resulting node network is shown in Figure 2.

2.2 Vehicle mobility

To model the PHEV movement in the network and the interaction of the vehicles with the energy system, the following elements need to be addressed: 1) the location of the vehicle in the grid (node number), revealing where the charging takes place; 2) the estimated remaining parking time of the vehicle at its present location, affecting how the vehicle should be charged, and 3) the estimated distance driven before the next grid connection, which also affects the charging process.

The cars travel within the city boundaries as determined by the node network. The number of PHEVs is 10,000, which corresponds to 3.6% of the cars in Helsinki [37] and enables the effects of the control strategies to be investigated without larger system constraints. The movement of each car is followed with 5-minute time steps. Selected key parameters are given in Table I. For the sake of simplicity, it is assumed that all the vehicles travel at a constant speed. It is also assumed that all the EVs in the system fully deplete their batteries before employing the internal combustion engine.

The movement of the vehicles in the node network is governed through two types of control functions, attraction and saturation functions. The task of the attraction function is to attract vehicles to certain nodes at certain times, whereas the saturation function determines when a vehicle is allowed to leave a specific node. Each vehicle is attracted only towards a predetermined single home node and work node and will see the rest of the home and work nodes as having zero attraction. Home and a work nodes are assigned to the vehicles semi-randomly; no correlation is assumed between the location of a single vehicle's home and work nodes, but the total number of vehicles assigned to each home and work node reflects the population statistics of Helsinki. The largest work node in the model can accommodate 1004 vehicles and the largest home node 162 vehicles.

The availability of a vehicle, i.e., the time a vehicle spends at a certain location, is described by a node type-specific monotonically growing saturation function $S_i(t) \in [0,1]$ and a vehicle-specific saturation factor $s_v \in [0,1]$. The requirement for a vehicle to leave is $S_i(t - t_{\mathrm{A},v}) \geq s_v$, where t is the current time and $t_{\mathrm{A},v}$ is the arrival time of the vehicle at the node. The exact departure time point t_{D} can be determined from the inverse of the saturation function: $S_i(t_{\mathrm{D}} - t_{\mathrm{A},v}) = s_v \Leftrightarrow t_{\mathrm{D}} = {S_i}^{-1}(s_v) + t_{\mathrm{A},v}$. In practice, when a vehicle v reaches node i, it is issued a random saturation factor s_v value from a distribution (here:

normal distribution restricted to between 0 and 1) and a timer variable $t_{\mathrm{T},v}$ that monitors the parking time (equivalent to $t - t_{\mathrm{A},v}$).

The saturation functions are based on expected behavior: here vehicles typically park for 0–2 hours at shopping and leisure nodes and 4–12 hours at home and work nodes. The maximum parking time is given by the time step that brings the saturation function S_i to 1. This maximum can, however, be exceeded if there are no available destinations for the vehicle after saturation. As an illustrative example, using a smooth S_i and a symmetrical normal-shaped distribution for the saturation factor, around x percent of the vehicles at a certain node become "saturated" (i.e., ready to leave) between parking times $[0, t_x]$, where $S_i(t_x) = \frac{x}{100}$.

Once the vehicle is saturated, the next destination is determined by the node-specific attraction functions $A_i(v,t) \geq 0$. These are designed to gravitate vehicles to places they are likely to be found at different times of day: e.g., around noon people are mostly at work, in the night they are at home, and in the late afternoon or early evening they are shopping.

To determine the next destination, we define a fitness value u_{ij} which is obtained by dividing the attraction function by the distance d_{ij} between the present node i and other nodes j:

$$u_{ij}(v,t) \equiv \frac{A_i(v,t)}{d_{ij}}, \quad i \neq j$$
$$u_{ii}(v,t) = 0 \tag{1}$$

where $A_i(v,t)$ is the value of the attraction function at node i for vehicle v at time step t.

These fitness indices are calculated for all nodes with nonzero attraction values. The destination is then chosen using fitness proportionate selection (a.k.a. roulette wheel selection). The fitness system is used to introduce variability in the routes, while still favoring shorter routes.

It should be noted that the fitness index values are independent of the charging-related parameters. Additionally, a separate random number stream is used for all vehicle movement-related randomness, such as assignment of the saturation factor. All the random number streams are reset between the simulation runs, making the movement of the vehicles identical in each run, and allowing a comparison of different cases with, e.g., different battery charging parameters.

The exact forms and values of the saturation and attraction functions are influenced by many factors, such as urban typology, infrastructure, available transportation options, gasoline prices, etc. But there are generally known time patterns and empirical profiles that can be used as a basis, as explained earlier. The control functions used in our analysis are shown in Figure 3.

2.3 Battery charging

It is assumed that all vehicles have identical batteries, so that only the current SOC may vary between different vehicles. The maximum battery charging rate is constant and determined by the capacity (see Table I). Batteries support any charging power between zero and the maximum charging rate and the SOC is directly proportional to the energy absorbed. Finally, all the cars are fully charged at home when the day begins.

In reality, these values vary greatly. For example, a real PHEV battery exhibits highly non-linear dynamics and the maximum charging rate depends on additional variables such as battery type, age, temperature, and SOC [20],[38],[39]. However, accounting for these would greatly increase the complexity of the model without providing substantial benefits on the system scale where 10,000 PHEV agents are simulated. Therefore, in order to maintain simplicity, these assumptions are appropriate.

The charging of a vehicle at a node that provides a grid connection is controlled by a charging control function Z that allocates power between the cars plugged into the node. This function could, in principle, include all the intelligence required to steer the interaction between the vehicle and the grid, e.g., accounting for limiting factors, such as the SOC of the vehicles at the node, battery power limitations, and estimated parking times. The complexity of the resulting control algorithm may vary, but the essential output is a vehicle-specific weight factor $w_{i,v}$, where $v \in V^i$ is a vehicle and V^i is the group of vehicles connected to node i.

The weight factors determine the power allocated to each vehicle, and thus have an important role in both maximizing the all-electric mileage and optimizing the electric mobility schemes within the local energy system. If the total available charging energy at the node is E_i, or alternatively, the maximum available power is P_i $(= E_i/dt)$, then the electricity allocated to a vehicle is equal to $w_{i,v} \times E_i$, or $w_{i,v} \times P_i \times dt$. Battery discharging into the grid could also be handled in a similar way, but this was not included in the study.

Two cases deserve special treatment. First, if the electricity allocated to the vehicle cannot be fully absorbed, e.g. because of the battery being at full SOC, this "overflown" energy is reallocated between the remaining vehicles in the node. Second, if the number of charging sockets at a node is less than the number of vehicles, some kind of queuing process will be necessary. To avoid this, it is assumed that there are as many sockets as vehicles at every node that supports charging.

Finally, the battery of each vehicle v at node i will be charged during a time interval dt with

$$\Delta E_v = \min\{\eta\, E_i^{\text{socket}}, Q_v - \text{SOC}_v, E_v^{\text{step}}, \eta\, w_{i,v} E_i\} \quad (2)$$

where E^{socket} stands for the socket limitation (here it is assumed 7.4 kW × 5/60 h ≈ 0.62 kWh, as a result of the use of 5-minute time steps), $Q_v - \text{SOC}_v$ for battery capacity limitation, E^{step} for battery charging limitation during one time step (so as not to exceed the battery's maximum recharging power; see Table I) and η is the charging efficiency, which is assumed to be 90% for all vehicles. The charging procedure is performed for all nodes at each time step, and is illustrated in Figure 4. The node may be subject to additional, possibly time-varying, energy system constraints that can be intermediated through simple power limitations of the type $\pm P_{\max}$.

The simple, no-control approach would be to value each car equally, i.e., each car would obtain the same charging power regardless of its status. Smart charging is defined here as an allocation scheme that does *not* value each car equally. Instead, it issues vehicle-specific weights based on vehicle-specific parameters such as SOC. The SOC of vehicles when parked is used here as the primary control parameter. For example, it would be intuitive to give preference to vehicles with a low SOC, in which case $Z^A = 1 - \widehat{\text{SOC}}$ (superscript A refers to the type of control strategy). However, when the intention is to have as many fully charged batteries as possible, then $Z^A = \widehat{\text{SOC}}$ would be the preferred choice.

While the total amount of allocated energy is node-specific, the weight factors of charging (at the node) are vehicle-specific and are obtained in the following way as normalized values of Z_v, the value of the charging function for vehicle v (e.g. $Z_v^A = 1 - \widehat{\text{SOC}}_v$):

$$w_{i,v} = \frac{Z_v}{\sum_{v \in V^i} Z_v}. \quad (3)$$

As the weight factors in Equation 3 are normalized values, the charging control functions need not be

unitless.

Two more sophisticated charging functions were also developed to incorporate the parking time and next free trip distance (the distance that the vehicle travels between different grid connections) into the control. The first one of these attempts to reach the highest traffic electrification while taking the finite charging opportunity window into account:

$$Z_v^B = \frac{Q_{\max} - \mathrm{SOC}_v}{\sigma\, T_v + \bar{T}(1-\sigma) + \delta(0)} \qquad (4)$$

where $Q_{\max}$ is the largest battery capacity among the vehicles at the node, T_v is the remaining parking time of the vehicle and $\bar{T}$ is the average remaining parking time for the current activity (e.g., working), calculated from departure time data obtained by running the trip generation algorithm once. $\delta(0)$ is a small number (here: 1) to avoid division with a zero denominator and finally, σ is a weight factor between prediction and average to account for the accuracy of the prediction of the parking time; if $\sigma = 0$ then the average car parking time is used, and if $\sigma = 1$ then an exact value is used (again, these are known when the trip generation algorithm is run once). The values of Z_v^B are in kilowatts.

The second control function seeks additionally to capture the effect of the distance to the next free charging point after leaving the present node. Note that the next free node is not necessarily the next node to which the car travels, as there may not be a charging opportunity, e.g., because of a lack of charging sockets. We combined three factors here: the SOC of the battery, the ability of the vehicle to manage the next trip with the current battery capacity, and finally a term that reflects on the remaining parking time:

$$\ln Z_v^C = \sigma_1\, \mathrm{SOC}_v + \sigma_2(D_v\, c - \mathrm{SOC}_v) - \sigma_3 \bar{P} T_v \qquad (5)$$

where D_v is the distance of the next free trip in kilometers, $\bar{P}$ is a power constant of 12 kW to match dimensions (it originates from the condition $\bar{P} \times 300\mathrm{s} = 1\ \mathrm{kWh}$), c is the unit electricity consumption of the vehicle in kilowatt-hours per kilometer, and the σ:s are the weighting factors for the three different components involved, given in inverse-kilowatt-hours. Z_v^C is thus in units of kilowatt-hours. The exponential form of Z_v is used here to avoid negative values. It should also be noted that the third term in Equation 5 is negative in order to prioritize those vehicles with the shortest parking time.

The above control functions contain the remaining parking time (T) and next free distance (D), both of

which need to be estimated. The remaining parking time T_v is obtained by predicting the remaining amount of time that a vehicle will stay at its current location:

$$T_v = \max(t_{0,\mathrm{D},v} - t + \delta\, r, 0) \qquad (6)$$

where $t_{0,\mathrm{D}}$ is the exactly known departure time step obtained by running the simulation once and t is the current time step. The term $\delta \times r$ represents the uncertainty in predicting the remaining parking time, where r is a normally distributed random number (mean value = 0, standard deviation = 1) and δ is an error parameter. A perfect prediction is obtained by setting $\delta = 0$. The average remaining parking time $\bar{T}$ for vehicles at a workplace is calculated from:

$$\bar{T} = \max(\overline{t_{0,\mathrm{D}}} - t, 0) \qquad (7)$$

where $\overline{t_{0,\mathrm{D}}}$ is the mean of the exactly known departure time steps from work.

The prediction of the distance of the next trip that the vehicle will take before the next charging session is calculated as

$$D_v = \max(D_{0,v} + \delta\, r, 0) \qquad (8)$$

where D_0 is the exactly known next trip distance (in kilometers) obtained by running the simulation once and $\delta \times r$ is the uncertainty in the prediction. As above, a perfect prediction is obtained by setting $\delta = 0$.

The metric used for measuring the effects from different charging strategies is the total distance driven in electric-only mode, or electric kilometers. A strategy is considered better than the alternative if it yields a higher total number of electric kilometers driven.

When there is ample power available for charging and the power distribution system is robust, the allocation method described above becomes irrelevant as it is easy to fully recharge each battery when needed. Figure 5 summaries the results of simulations based on the above approach to determine the conditions where smart charging could make a difference. Two parameters were used: battery capacity and unit power available at a node (referred to as the *power coefficient*, which is defined as the total power available at the node divided by the number of vehicles that are assigned to the node); other parameter values used in the simulations are given in [40]. Figure 5 implies that the power coefficient would need to be limited down to around 0.1 kW in order to obtain visible differences in all-electric mileage between competing charging strategies. This value was used in the simulations that follow.

3. Results

The model described above is generic and can be used for different sites and conditions. The control strategies described above were tested in an environment representing Helsinki metropolitan region (Finland). With the resulting travel distance distributions, 90% of the PHEV fleet could manage the journeys using electricity only if the battery capacity is larger than 7 kWh.

The aggregated charging power for this case is shown in Figure 6 for two different simulation runs with a morning peak when cars are parked at work (left) and with an early evening peak at home nodes (right). The morning peak could easily be smoothed out (from 6 to 1 MW) through limiting charging power to 0.1 kW $\times N$ (where N is the number of cars assigned to the node) from the non-limited power value. Though the peak power amounts to 11 MW, the total electricity needed to operate the 10,000-car fleet remains at only 30 MWh.

However, the aggregated load profile fails to illustrate the spatial differences between work and home charging peaks. To address this, Figure 7 shows the spatial charging power in the city during the peaks when no smart control is exercised. It can be seen that the work peak is caused by a few nodes charging at high power, while the home peak is caused by a large number of nodes charging at lower power: the highest peak among all the work nodes is 0.63 MW (the workplace of 1,000 cars) and among home nodes, the highest peak is 0.19 MW (the home of 131 cars).

Without any predictions about the future, a reasonably good charging strategy proved to be based on an exponential form of the SOC of the battery, or $\ln Z = \alpha$ SOC, where α is a weighting coefficient. Figure 8 shows the increase in all-electric mileage with this strategy compared to the case where all cars are weighted equally (dumb charging), with different weights α and different battery capacities. For very small battery capacities (less than 2 kWh), it is best to allocate more power to vehicles with a high SOC. For higher capacities, favoring a low SOC yields a better result. For capacities higher than 8 kWh, this strategy has little effect compared to an equal distribution strategy. The reason for the inversion at 2 kWh is presumably that the charging function allocates too much power to low-priority vehicles that have just arrived at the node (because the battery is near-empty), ignoring the high-priority vehicles that have already spent some time at the node and are thus likely to depart sooner.

Adding more intelligence to the charging process requires further knowledge about the intended travel pattern in order to obtain full benefit from the more sophisticated allocation functions in Equation 4 and

Equation 5. A comparison of the charging control against dumb charging is shown in Figure 9. A linear SOC-based control (Z^A) yields an improvement of around 1% at most. With complete knowledge of the travel pattern, a more sophisticated control strategy (Z^C) would yield an improvement of up to 5.5% (with a 2.5-kWh battery) in the all-electric mileage, but this is heavily dependent on the battery size, as shown in Figure 9. Though these numbers may sound modest, it should be observed that the upper limit (not necessarily the lowest upper limit) of increased all-electric mileage is 11% when the node total power limitation is removed, meaning that, e.g., here the Z^C strategy represents here >50% of the "maximum" value. The "maximum" increase of 11% may not be attainable even with a perfect charging function.

When sophisticated control strategies are being implemented, the accuracy of the predicted travel schedule for the vehicles is an important question as this will affect the way they are charged. To study the influence of the prediction accuracy of parking time and distance driven before next grid connection, we simulate each day twice so that a perfect prediction could be produced for the second run from the first one. A Gaussian error is then added to this driving statistic. The error of the prediction is measured as multiples of one sigma (expressed in hours or kilometers): a 1-hour prediction error then means that around 68% of the EVs depart within ±1 hour from the predicted time value.

Figure 10 demonstrates how the prediction inaccuracy in parking time will affect the benefits from intelligent charging strategies (Z^B) with two battery sizes (2 and 10 kWh). The prediction error is shown as a parameter ranging from 0 to ~ ∞ (in Figure 10, set to equal 1000) hours. The horizontal axis describes the weight of the prediction: a value of 0 means that one and the same average departure time is used for all cars, and a value of 1 means that the parking time used in the weight calculations is the predicted parking time. We observe that with a perfect prediction (error = 0 hours) the extra electric kilometers gained over no control strategy increase monotonically when moving toward predicting each car's parking time individually instead of using the average value; a gain of around 3.5% was obtained. However, the gain drops quickly with increasing prediction error, e.g., a 2-hour error halves the gain and it vanishes almost completely at 8 hours. At large error values (>4 hours) a combination of individual and average parking times seems to yield an optimum. With very high prediction errors, abandoning the predictive control yields the best outcome. Another observation is that, with a small or large battery capacity compared to the average travel distance per day, the positive effects of predicting decrease. For example, with a 10-kWh battery the travel requirements can almost always be fulfilled through electricity, regardless of any prediction inaccuracy which leads to insignificant gains from any control

strategy. In our case the highest impacts were obtained at a capacity of around 2 kWh.

Using the most sophisticated control strategy Z^C from Equation 5 instead of Z^B, used in Figure 10, would yield a 5% improvement in all-electric mileage with a 2-kWh battery, assuming perfect predictions. In Figure 11, we analyzed this case further in terms of varying the weight of the prediction of two parameters in Z^C, the parking time and the next free distance, assuming a perfect prediction. The weight of SOC (σ_1) was set to 0 (with a weight of 0, a parameter is removed from Z^C). It is observed that, if there is information available on the next driving distance only and no information about the parking time (weight of parking time prediction = 0), the smart control strategy would increase the electric kilometers by 1%. In the opposite case (weight of next free distance = 0), Z^C yields an increase of around 4.5%. If we weighted both parameters optimally in Z^C, this would yield a slightly better result or a 5% improvement at the optimum shown in Figure 11. Negative weight values were also tested to verify that a sensible strategy will favor vehicles with longer rather than shorter free distances, and shorter rather than longer parking times.

4. Conclusions

The results show that smart control strategies with predictive elements could lead, in the case of Helsinki, to an increase of over 5% in the all-electric mileage compared to a no-control (equal power allocation) strategy. Achieving this requires an accurate prediction of the remaining parking time and the distance the vehicle will travel before the next grid connection. The results also indicate that, with a very high prediction error, with a very small or large battery, or with abundant charging power, smart charging control would not bring considerable benefits. Thus, the potential of smart charging to increase the all-electric mileage seems limited. As a matter of fact, a charging strategy based on, e.g., "dumb" equal power allocation may be adequate. Moreover, this could provide positive benefits for the power system, e.g., to increase the flexibility of smart grids, without jeopardizing the all-electric mileage of PHEVs.

It should be observed that simplifying assumptions have been used in the trip generation and charging models, which may affect the results. Therefore, the conclusions should be regarded as indicative only.

References

[1] Fulton L, Cazzola P, Cuenot F, Kojima K, Onoda T, Staub J, et al. Transport, Energy and CO2: Moving Toward Sustainability. Paris, France: OECD/IEA. 2009.

[2] De Almeida P, Silva PD. The peak of oil production—Timings and market recognition. *Energy Policy* 2009; **37**(4):1267–1276, DOI:10.1016/j.enpol.2008.11.016.

[3] International Energy Agency. Technology Roadmap: Plug-in and Electric Vehicles. Paris: OECD/IEA. 2011.

[4] Edwards R, Mahieu V, Griesemann J-C, Larive J-F, Rickeard DJ. Well-to-wheels analysis of future automotive fuels and powertrains in the European context. *SAE transactions* 2004; **113**(4):1072–1084 Available: http://cat.inist.fr/?aModele=afficheN&cpsidt=16973492. Accessed 12 Feb 2013.

[5] Koch AK, Fowler MW, Fraser RA. Implementation of a fuel cell plug-in hybrid electric vehicle and factors affecting transportation policy. *International Journal of Energy Research* 2011; **35**(15):1371–1388, DOI:10.1002/er.1907.

[6] Ahlgren EO, Börjesson M. Assessment of transport fuel taxation strategies through integration of road transport in an energy system model — the case of Sweden. *International Journal of Energy Research* 2012; **36**(5):648–669, DOI:10.1002/er.1824.

[7] Jun E, Jeong YH, Chang SH. Simulation of the market penetration of hydrogen fuel cell vehicles in Korea. *International Journal of Energy Research* 2008; **32**(4):318–327, DOI:10.1002/er.1358.

[8] Kempton W, Tomić J. Vehicle-to-grid power implementation: From stabilizing the grid to supporting large-scale renewable energy. *Journal of Power Sources* 2005; **144**(1):280–294, DOI:10.1016/j.jpowsour.2004.12.022.

[9] Kempton W, Tomić J. Vehicle-to-grid power fundamentals: Calculating capacity and net revenue. *Journal of Power Sources* 2005; **144**(1):268–279, DOI:10.1016/j.jpowsour.2004.12.025.

[10] Mets K, Verschueren T, Haerick W, Develder C, De Turck F. Optimizing smart energy control strategies for plug-in hybrid electric vehicle charging. *2010 IEEE/IFIP Network Operations and Management Symposium Workshops*. IEEE, 2010; 293–299, DOI:10.1109/NOMSW.2010.5486561.

[11] Clement K, Haesen E, Driesen J. Coordinated charging of multiple plug-in hybrid electric vehicles in residential distribution grids. *2009 IEEE/PES Power Systems Conference and Exposition*. IEEE, 2009; 1–7, DOI:10.1109/PSCE.2009.4839973.

[12] Zhang Q, Ishihara KN, Mclellan BC, Tezuka T. An analysis methodology for integrating renewable and nuclear energy into future smart electricity systems. *International Journal of Energy Research* 2012; **36**(15):1416–1431, DOI:10.1002/er.2948.

[13] Guille C, Gross G. The integration of PHEV aggregations into a power system with wind resources. *2010 IREP Symposium Bulk Power System Dynamics and Control - VIII (IREP)*. IEEE, 2010; 1–9, DOI:10.1109/IREP.2010.5563263.

[14] Galus MD, La Fauci R, Andersson G. Investigating PHEV wind balancing capabilities using heuristics and model predictive control. *IEEE PES General Meeting*. IEEE, 2010; 1–8, DOI:10.1109/PES.2010.5589267.

[15] Zhou C, Qian K, Allan M, Zhou W. Modeling of the Cost of EV Battery Wear Due to V2G Application in Power Systems. *IEEE Transactions on Energy Conversion* 2011; **26**(4):1041–1050, DOI:10.1109/TEC.2011.2159977.

[16] Peterson SB, Apt J, Whitacre JF. Lithium-ion battery cell degradation resulting from realistic vehicle and vehicle-to-grid utilization. *Journal of Power Sources* 2010; **195**(8):2385–2392, DOI:10.1016/j.jpowsour.2009.10.010.

[17] Guerin JT, Leutheuser A. Vehicle integration issues for hybrid energy storage systems. *International Journal of Energy Research* 2010; **34**(2):164–170, DOI:10.1002/er.1656.

[18] Kempton W, Udo V, Huber K, Komara K, Letendre S, Baker S, et al. A Test of Vehicle-to-Grid (V2G) for Energy Storage and Frequency Regulation in the PJM System. 2008.

[19] Galus MD, Waraich RA, Andersson G. Predictive, distributed, hierarchical charging control of PHEVs in the distribution system of a large urban area incorporating a multi agent transportation simulation. *Proc. 17th Power Systems Computation Conf.* Stockholm, Sweden, 2011.

[20] Su W, Chow M-Y. Computational intelligence-based energy management for a large-scale PHEV/PEV enabled municipal parking deck. *Applied Energy* 2012; **96**:171–182, DOI:10.1016/j.apenergy.2011.11.088.

[21] DeForest N, Funk J, Lorimer A, Ur B, Sidhu I, Kaminsky P, et al. Impact of Widespread Electric Vehicle Adoption on the Electrical Utility Business – Threats and Opportunities. 2010 Available: http://ikhlaqsidhu.files.wordpress.com/2010/03/nr_utilities_final_8-31-09.pdf. Accessed 12 Feb 2013.

[22] Pillai JR, Bak-Jensen B. Impacts of electric vehicle loads on power distribution systems. *2010 IEEE Vehicle Power and Propulsion Conference*. IEEE, 2010; 1–6, DOI:10.1109/VPPC.2010.5729191.

[23] Huo H, Zhang Q, Wang MQ, Streets DG, He K. Environmental implication of electric vehicles in China. *Environmental Science & Technology* 2010; **44**(13):4856–61, DOI:10.1021/es100520c.

[24] Neubauer J, Brooker A, Wood E. Sensitivity of battery electric vehicle economics to drive patterns, vehicle range, and charge strategies. *Journal of Power Sources* 2012; **209**:269–277, DOI:10.1016/j.jpowsour.2012.02.107.

[25] Moura SJ, Callaway DS, Fathy HK, Stein JL. Tradeoffs between battery energy capacity and stochastic optimal power management in plug-in hybrid electric vehicles. *Journal of Power Sources* 2010; **195**(9):2979–2988, DOI:10.1016/j.jpowsour.2009.11.026.

[26] Oliveira DQ, Zambroni de Souza AC, Delboni LFN. Optimal plug-in hybrid electric vehicles recharge in distribution power systems. *Electric Power Systems Research* 2013; **98**(May):77–85, DOI:10.1016/j.epsr.2012.12.012.

[27] Gan L, Topcu U, Low SH. Optimal Decentralized Protocol for Electric Vehicle Charging. *IEEE Transactions on Power Systems* 2013; **28**(2):940–951, DOI:10.1109/TPWRS.2012.2210288.

[28] Sheikhi A, Bahrami S, Ranjbar AM, Oraee H. Strategic charging method for plugged in hybrid electric vehicles in smart grids; a game theoretic approach. *International Journal of Electrical Power & Energy Systems* 2013; **53**:499–506, DOI:10.1016/j.ijepes.2013.04.025.

[29] Galus MD, Andersson G. Demand Management of Grid Connected Plug-In Hybrid Electric Vehicles (PHEV). *2008 IEEE Energy 2030 Conference*. Atlanta, Georgia: IEEE, 2008; 1–8, DOI:10.1109/ENERGY.2008.4781014.

[30] Vasirani M, Ossowski S. A proportional share allocation mechanism for coordination of plug-in electric vehicle charging. *Engineering Applications of Artificial Intelligence* 2013; **26**(3):1185–1197, DOI:10.1016/j.engappai.2012.10.008.

[31] Kiviluoma J, Meibom P. Methodology for modelling plug-in electric vehicles in the power system and cost estimates for a system with either smart or dumb electric vehicles. *Energy* 2011; **36**(3):1758–1767, DOI:10.1016/j.energy.2010.12.053.

[32] Galus MD, Andersson G. Balancing Renewable Energy Source with Vehicle to Grid Services from a Large Fleet of Plug-In Hybrid Electric Vehicles controlled in a Metropolitan Area Distribution Network. *Symp. of Int. Council on Large Electric Systems*. Bologna, Italy, 2011 Available: http://www.future-energy.ethz.ch/uploads/tx_ethpublications/Cigre_Bologna_MG_full.pdf.

[33] Rautiainen A, Repo S, Mutanen A, Vuorilehto K, Jalkanen K. Statistical Charging Load Modeling of PHEVs in Travel Survey Data. *IEEE Transactions on Smart Grid* 2012; **3**(4):2004–2005, DOI:10.1109/TSG.2012.2206411.

[34] G4V - Grid for Vehicles. 2011 Available: http://www.g4v.eu.

[35] Map of Helsinki. 2010 Available: http://maps.google.com. Accessed 15 Oct 2010.

[36] Dijkstra EW. A note on two problems in connexion with graphs. *Numerische Mathematik* 1959; **1**(1):269–271, DOI:10.1007/BF01386390.

[37] City of Helsinki: City Planning Department. Liikenteen kehitys Helsingissä vuonna 2011 (The Development of Transportation in Helsinki in 2011). 2012 Available: http://www.hel2.fi/ksv/julkaisut/esitteet/esite_2012-2.pdf.

[38] Su W, Chow M-Y. Sensitivity analysis on battery modeling to large-scale PHEV/PEV charging algorithms. *IECON 2011 - 37th Annual Conference of the IEEE Industrial Electronics Society*. IEEE, 2011; 3248–3253, DOI:10.1109/IECON.2011.6119831.

[39] Reddy TB, Linden D. Linden's Handbook of Batteries. 4th ed. New York: McGraw-Hill. 2011.

[40] Lindgren J, Niemi R, Lund PD. PV-to-EV Schemes for Photovoltaics Integration and Power Balance. *Proceedings of the 2nd International Workshop on Integration of Solar Power into Power Systems*. Lisbon, Portugal, 2012; 1–8.

TABLES

Table 1. Selected simulation parameters and their values.

Parameter(s)	Value range	Comments
EV battery capacity	1-10 kWh	Shared by all vehicles.
EV unit consumption	0.2 kWh/km	Shared by all vehicles.
EV charging efficiency	90%	Shared by all vehicles.
EV speed	60 km/h	Shared by all vehicles. Traffic congestion is not modelled.
Max charging power (socket)	7.4 kW	2 × 16 A at 220 V
Max charging power (battery)	P kW	P is equal to the battery capacity in kilowatt-hours, resulting in a 60-minute charging time from empty to full, assuming other limitations are not exceeded.
Average EV travel	24.3 km/day	Obtained from measured drive cycles

distance		(output parameter).
Standard deviation of EV travel distance	12.3 km/day	Obtained from measured drive cycles (output parameter).
Other charging limitations	*	Adequate sockets at home and work nodes. Charging not possible at other nodes. Total charging power at a node may be limited.

FIGURES

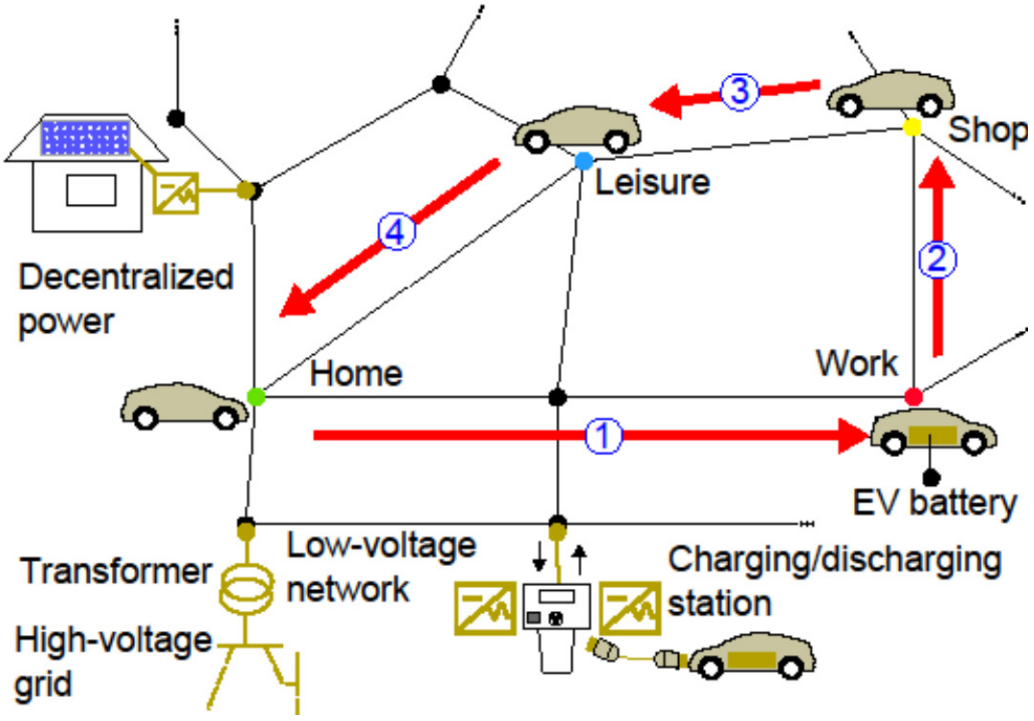

Figure 1. Schematic illustration of the road and electric network infrastructure. The daily route of an electric vehicle (1-2-3-4) is also depicted.

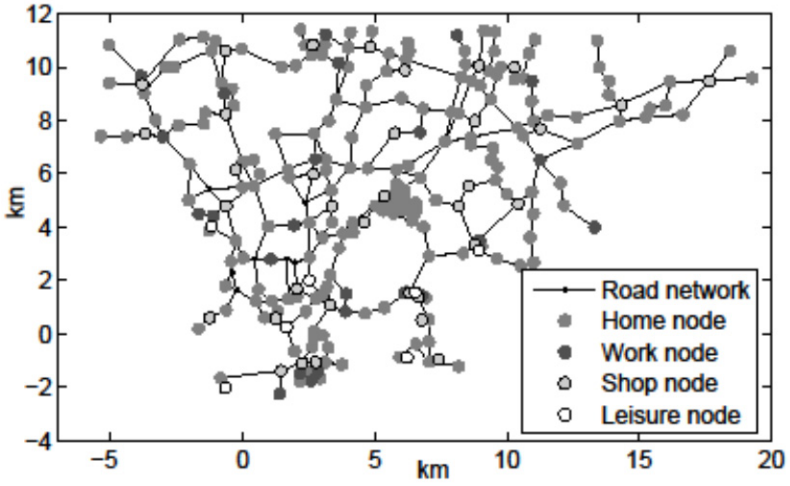

Figure 2. Node network representing Helsinki used in the simulations.

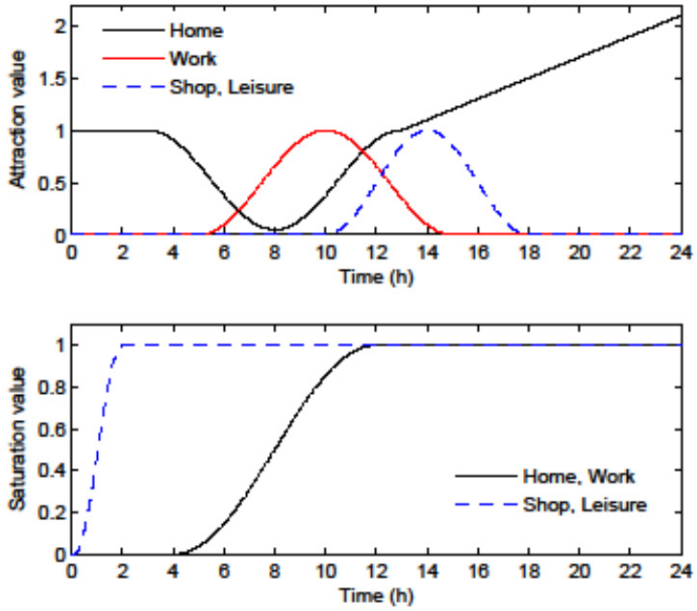

Figure 3. Control functions used in the simulations.

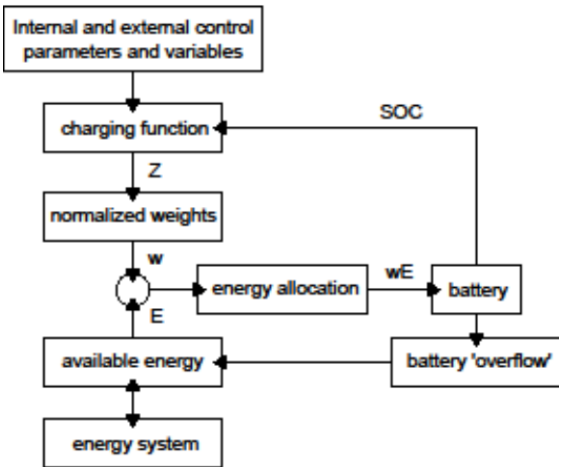

Figure 4. Battery charging algorithm.

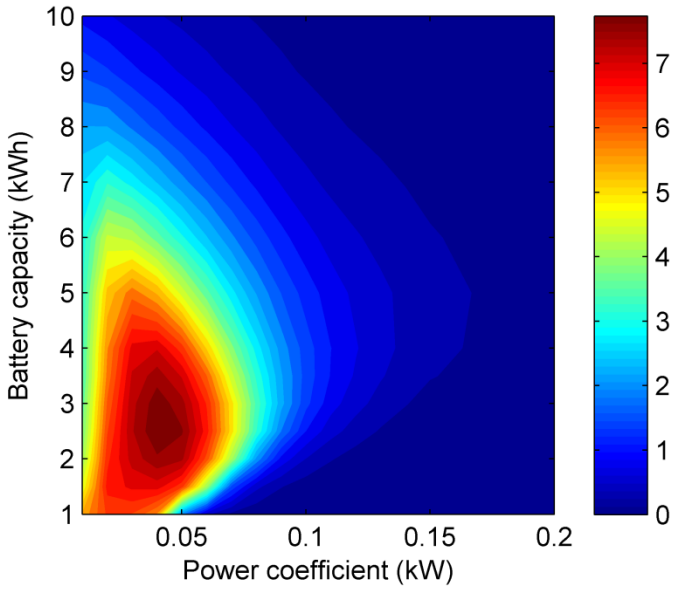

Figure 5. Increase in electric mileage (%) as a result of smart charging with different battery capacities and power coefficients.

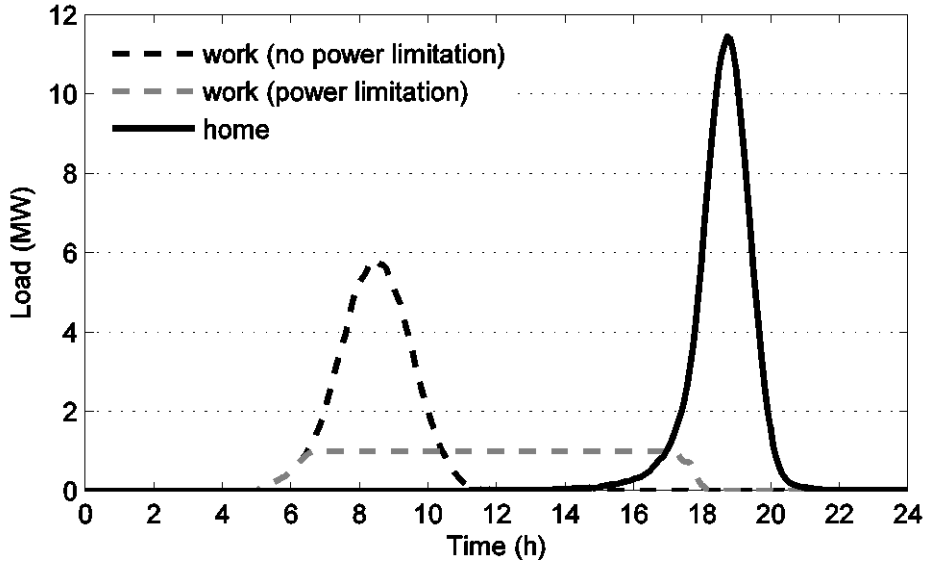

Figure 6. Total charging power for 10,000 PHEVs in Helsinki with and without charging power limitations. The total charging power limitation applies at work nodes and is equal to 0.1 × N kW, where N = the number of cars assigned to the workplace.

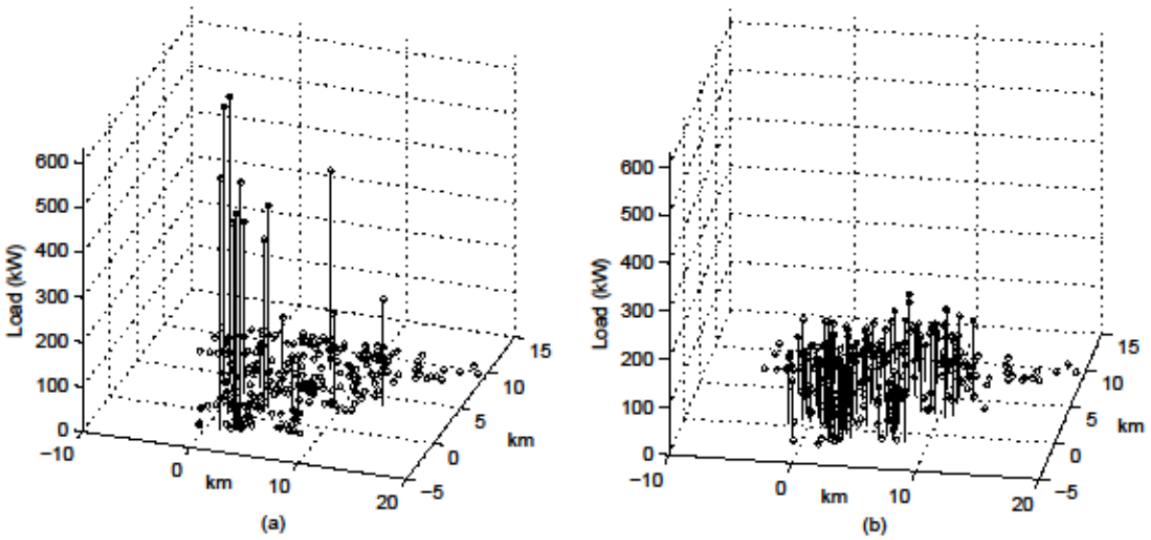

Figure 7. Spatial charging power distribution for 10,000 PHEVs in Helsinki at 8:30 a.m. (charging peak at work, Figure 4a) and at 6:45 p.m. (charging peak at home, Figure 4b) without total charging power limitations.

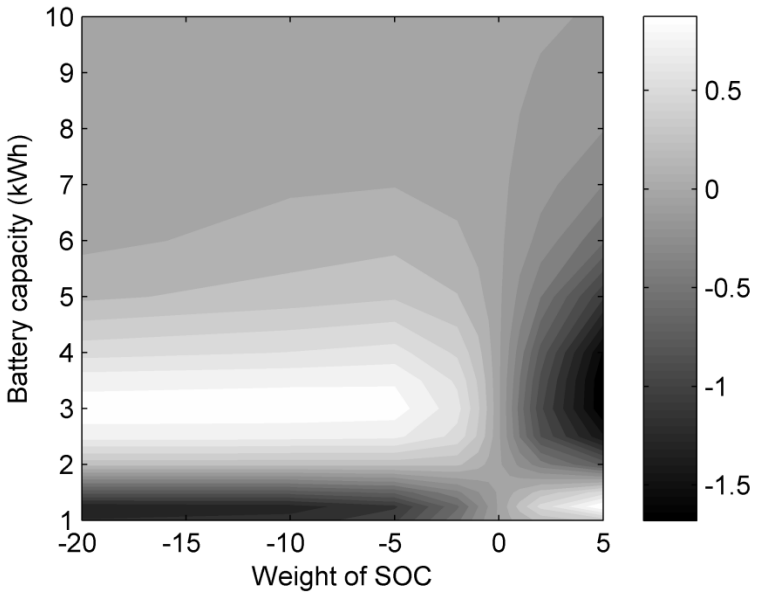

Figure 8. Increase in electric mileage (%) as a function of weight of SOC α and battery capacity using the charging function $Z = \exp(\alpha \text{ SOC})$.

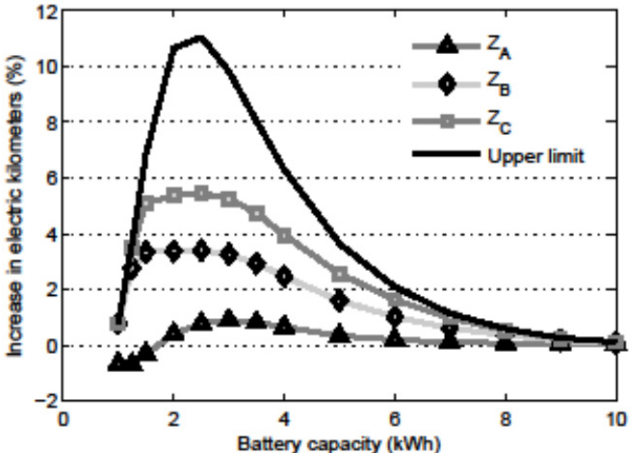

Figure 9. Gain in electric mileage using different charging strategies (Z^i) versus battery capacity for the Helsinki case with 10,000 vehicles. In strategy Z^B (Equation 4), $\sigma = 1$. In strategy Z^C (Equation 5), $\sigma_2 = 0$, $\sigma_3 = 1$ and σ_1 is optimized to the integer value that yields the highest number of electric kilometers for the current capacity.

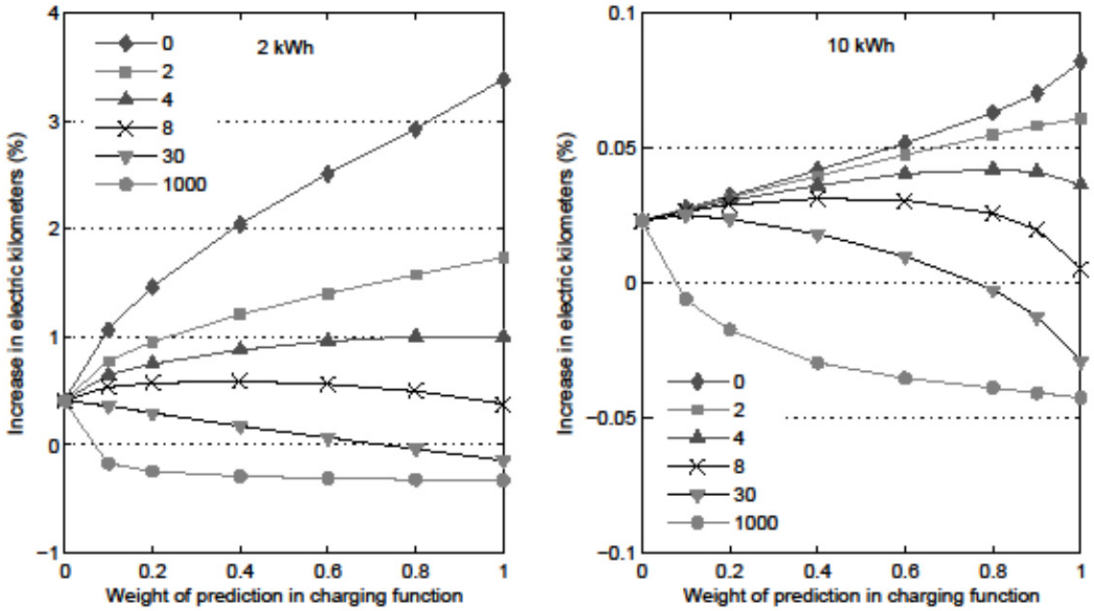

Figure 10. Effect of parking time prediction on the electric kilometers with different prediction errors (in hours) and battery capacities. The horizontal axis depicts the linear combination of observed average parking time and the prediction of the parking time individually (0 = average, 1 = prediction). Smart control strategy Z^B (Equation 4) is used.

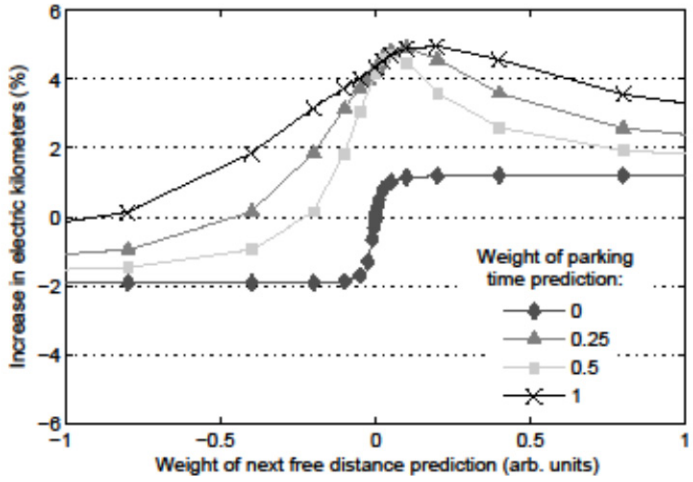

Figure 11. Effect of weighting parking time and next free distance on electric kilometers in smart control strategy Z^C (Equation 5). 2-kWh battery capacity and perfect predictions (parking time error=0 h, next free distance error=0 km).